Finite Element Method Validity on Biconic Cusp Magnetic Confinement

Jonathan Kelley

June 3, 2017

1 Abstract

Energy generation through nuclear fusion has been a focus of research for several decades. One such concept employs inertial electrostatic confinement of charged ions, accelerating fusion fuel with sufficient kinetic energy to satisfy the lawson criterion. This concept was analyzed using the finite element method using the EMWorks FEM pacakge for SOLIDWORKS, with a focus on magnetic and electrostatic field interactions in a biconic and quasipsherical cusp system. The SOLIDWORKS model was then used to construct a physical system with according characteristics. An analysis was performed measuring the magnetic field of the physical model with comparison to the finite element model. A single and dual coil biconic cusp system was constructed to match the SOLIDWORKS model specifications and tested with a hall effect magnetic field probe. The results proved that the β field behavior of the FEM model was indeed similar to the experimental devices. However, continual development of the FEM model and coil construction is required to numerically validate the FEM model for use in inertial electrostatic confinement fusion.

2 Introduction

Nuclear fusion with the aim of generating usable electric power has undergone significant research for several decades [20]. According to Ongena and Ogawa, nuclear fusion is appealing as a new source of power because of its desirable environmental considerations and virtually inexhaustible fuel supply [15]. There are currently many different strategies for generating the fusion conditions required for efficient atomic nuclei reactions. Some systems involve containing a heated plasma while others focus on bringing solid fuel to ignition conditions. This paper explores the design of the electromagnetic coils for fusion systems with the unique characteristic of a combination electrostatic and magnetostatic fuel acceleration. The β fields are studied in depth against a new finite element method that allows for rapid iteration and design in the SOLIDWORKS software package.

Modern research in the development of nuclear fusion devices follows two main strategies. The first strategy involves the use of magnetic fields to contain a very energetic dense plasma of light atomic nuclei[14]. This approach is commonly found in systems like stellerators and tokamaks such as the Wendelstein 7-X project in Germany and the ITER project in France. A second approach follows inertial confinement of a solid fuel pellet that is heated to fusion conditions by a laser or ion beam [4]. This technique has been successfully demonstrated in the National Ignition Facility at the Lawrence Livermore National Laboratory. While these techniques have been moderately successful, there are several other methods of achieving fusion conditions with the intent to generate electrical energy.

Of the other various nuclear fusion strategies, the formation of a potential well through the confinement of electrons has shown promising results. EMC2 has reported neutron emission of 1E9 fus/sec [19] with a quasi-spherical magnetic trap and ionized deuterium injection. The potential well created by magnetic cusp confinement of electrons generates substantial electric potential for the positively charged deuterium gas to reach sufficient kinetic energy for fusion. One such device that utilizes this strategy is the Polywell fusor. The Polywell system is an improvement on traditional electrostatic confinement as there are no electron losses due to conduction with physical cathode. The electrical potential as generated by the confined electrons serves as a "virtual cathode," accelerating the fuel ions.

Despite being an adequate solution for conduction losses, the official Polywell design [8] continues to struggle from losses due to bremsstrahlung radiation [3], conduction losses to unshielded construction [16], and cusp losses [11] by electron leakage [2]. In the 1991 paper on electron leakage, Bussard describes that cusp losses constitute the majority of losses in the simulated Polywell system. Conduction losses to joints and unshielded surfaces contributed the majority of loss for the early Polywell design, but this was identified and rounder solenoids and shielding was implemented to mitigate conduction effects [8]. It is estimated that no more than 3E-5 fractional surface area of the machine can be unshielded to fully mitigate conduction losses [19]. Electron leakage through point cusps

generated by the magnetic field serves as the current major loss mechanism for Polywell theory[19].

As electron leakage from the containment field is the major contribution to cusp loss, it is important to identify the factors that lead to poor confinement. There are several aspects to quasi-spherical magnetic trapping that impact efficiency and potential well depth. Efficiency when concerning this system relates the amount of electrons injected into the well and the depth of the well itself. Systems that do not trap the electrons for a substantial amount of time will be much more inefficient as more electrons are required to maintain the well. The electrons lost in this system are predicted and verified to escape through point cusps generated by parallel magnetic fields located in near the vertexes and face centers of the quasi-spherical system. In a complete cubic Polywell system, this corresponds to 27 point cusps [5] and 10 linear cusps when spaced far apart. The classic biconic cusp system has only two point cusps and a very large ring cusp along the mid plane of the two electromagnets. It has been found that linear and ring cusps contribute to the majority of loss for a Polywell system [17], however attempts to reduce such cusps in favor of more point cusps has only demonstrated a very small improvement. This is because electron loss is proportional to the total amount of point cusps in the system. Despite the similar loss rates, confinement time of electrons was increased by 2.5 times that of the standard 27 point cusp system [18]. While the losses and transit times associated with the point cusps are easier to calculate, the cusps created by coils spaced less than their critical distance are much more complicated and thusly named "funny cusps." It is key when designing a magnetic trapping system to minimize spacing between coils as the complex cusps are eliminated. In addition to minimzing loss, recent simulations have also demonstrated an increased transit time for electrons entering the null point [13]. This is valuable as per the Lawson Criteria [12] where greater confinement time increases the likelihood of fusion.

Despite the realization that high beta confinement increases the potential well in a Polywell system, the plasma must first enter low beta and experience similar loss mechanisms. There have been several studies that successfully model electron trajectory in a low beta systems because electrostatic effects between the electrons is ignored; the plasma pressure is low enough to assume independent particle motion[13, 5, 6]. Ultimately, a Polywell system with reduced loss will consist of high beta plasma confinement and the reduction of point cusps. This will increase electron density and minimize loss due to poor cusp confinement [8]. A major point of interest is reducing losses due to point and line cusps generated by coil arrangement. There are several ideas that involve electrostatic repulsion as a virtual barrier to electrons escaping through point and line cusps. In a traditional magnetic mirror system, plasma is confined axially symmetric through two sets of electromagnetic coils. However, the charged particles of the plasma follow the magnetic field lines and expand in the space between the coils [1]. Early researchers implemented Joeffe bars as a way to stabilize plasma in this region, but it was determined that Joeffe bars do not completely close ring cusps, but rather form sets of linear cusps [17]. In addition, the geometry of the

Joeffe bars does not integrate with the quasi-spherical polyhedron arrangement of the confinement coils.

The second theory of eliminating point cusp loss is through the use of electrostatic repeller plates that generate an electric field barrier. In a low beta environment, point cusp loss can be modeled by the Child-Langmuir law and the amount of power lost can be estimated. While repeller plates demonstrate loss in theory, they have not yet been proven to adequately reduce electron loss [5]. Dolan explored the concept of penning traps and electrostatic plugging in a magnetic confinement system with traditional plasma behavior. However, it is noted that the Polywell and penning trap systems would benefit from electrostatic plugging despite inadequate performance on spindle cusp systems[7]. However, it is noted that repeller plates would suffer from conduction losses if placed within an effective range for the point cusps. Despite this, the concept of electrostatic plugging remains a valid solution to reducing point cusp losses. A simulation by an Australian research team includes both magnetic and electrostatic fields contained within the device with the electric field source centered about the coil geometry [10]. The resulting structure is a combination of classic insulating magnetic coils and an external electric field that generates a mirror electric point cusp within the coil face to prevent electron loss.

In a hybrid system that combines electric and magnetic fields as described in the Sydney experiment, the confinement time of electrons is increased. Due to the addition of the electric field, the strength of the virtual anode is significantly increased and more energy is transferred to the ion fuel, raising the rate of fusion. The virtual cathode generated by electrons in the magnetic confinement system works in tandem with a new virtual anode generated by the electric field. Currently, this is the only study that investigates the combination of electric fields and magnetic fields in a biconic cusp configuration with high fidelity. If the same concept involving electrostatic acceleration is to be applied to high-performance cusp devices like the Polywell, then the independent field interactions must modeled on a system with associated geometry.

There are several methods of analyzing magnetostatic and electrostatic field interactions. Multiphysics programs and magnetic field modeling tools are very capable of preforming the required calculations to analyze the complicated cusp geometries of the biconic cusp and Polywell systems, but are not well suited for the iterative engineering design process. Many parameters like wire gauge, heat dissipation, shell thickness, and specific torus characteristics are either ignored or heavily simplified. A powerful engineering tool is the finite element method, a way of approximating values of equations related to thermodynamics, structural analysis, and field potentials for complicated geometries. The advantage of using the finite element method in coil design is the ability to quickly iterate and optimize the system geometry. This method also allows the ability to switch between a very coarse approximation for large geometry changes and a fine approximation for tuning very specific field interactions.

The goal of this project is to employ the finite element method in designing a single coil and biconic cusp system with intent for use in nuclear fusion research. Three spherically contained models will be developed for this analysis: a single

coil, a biconic cusp dual-coil, and a quasi-spherical Poylwell geometry. Each model will be developed using parametric design in SOLIDWORKS and then analyzed using the EMWorks FEM magnetostatic solver. Once the analysis is complete, a physical model will be constructed and the magnetic field will be measured for comparison with the FEA results.

3 Methods

A computational model must first be developed before any experimental data can be collected and analyzed. Because electron confinement time is the primary metric for determining the effectiveness of the addition of the electric field, a simulation utilizing an electron orbit theory model will be performed to determine an optimal device construction parameters. As electron confinement time is directly related to the strength of the associated trapping magnetic fields[13], the model will focus primarily on mapping the respective B and H values at set points around the coil. Individual parameters specific to each system will be altered and data on the B and H fields collected from the FEM models will be graphed according to their distance and elevation from the device origin. By reducing individual data points to their distance and elevation, data collection is greatly simplified. These data will be sufficient to verify the validity of the FEM model for design and engineering, but not comprehensive enough for analysis of a system with time-variant parameters.

3.1 Simulation Overview

The first step in analyzing coil design for use in electron confinement devices is to create a three-dimensional model that can be meshed and calculated for use in a finite element tool. SOLIDWORKS will be selected as the modeling tool because of its strength in parametric design and extensive simulation packages. The FEM package used will be EMWorks which is an add-on that allows extensive control over model meshing, boundary conditions, and data collection. EMWorks has the ability to seamlessly integrate with SOLIDWORKS modeling software and is specialized for magnetostatic and electrostatic cases. Two types of magnetostatic data will be collected: the β field surrounding the coil and its strength H. The β field represents the magnetic field without reference to the charge of the object to which it is interacting. This data is specifically useful because a direct comparison can be made with the physical model as real-world data will be collected using a magnetic field sensor operating in millitesla. The H field is more representative of the forces acting on the individual electrons entering the β field which is useful in the context of this project.

The accuracy of the model will be directly related to the mesh quality, boundary condition selection, and non-metal dieletric modeling. Perhaps the most deterministic parameter in this system will be the mesh quality or "fineness" of the individual elements that make up the mesh body. With the given physical scale of the project, it might be too computationally intensive to collect accurate

and precise data in specific regions of interest without selecting regions where coarser meshing is appropriate. In the more complicated geometries beyond the single coil experiment, early tests demonstrated the need for "mesh region isolation," where the β field in specific areas of interest in the mesh are calculated with a greater fineness. This is important because the early behavior of the β field interactions did not show the presence of any cusp formation.

It is expected, in both the physical and model simulations, that the β field will follow the general form of β from a current carrying wire with respect to the Biot-Savart law. Mathematically this is represented as:

Where β is measured on plane

$$\beta = N\frac{\mu_0 I}{2R}$$

and where β is measured on z above the loop plane

$$\beta = N\frac{\mu_0 2\pi R^2 I}{4\pi\left(z^2+R^2\right)^{3/2}}$$

where R is the radius of the coil, N is the number of turns, I is the current through each wire, and μ_0 is the permeability of free space for the selected medium. In the case of this project, μ_0 will be $1.257E^{-6}\ T\cdot m/A$, equal to magnetic permeability of air. Therefore, as z increases, it is expected that β will decrease. In addition, as the current through the wires increases, so should β. Also from these formulae it can be concluded that larger coils will generate smaller β fields, or that smaller coils will generate larger β fields given the same input parameters.

Larger coils have the advantage of being able to contain and dissipate more heat than smaller coils, but have less efficiency due to resistive power losses over the increased length. Larger coils are desirable in biconic cusp fusion as fusion power scales to the seventh power of the coil radius under ideal conditions [9]. In order to make the physical model feasible to construct with a relatively small budget, coil radii between 5 and 8 cm will be used for optimization with coil thickness as 20% of the radius. This thickness value was chosen due to the sizes of available materials for construction of the physical systems.

3.2 Experimental Overview

Construction of the physical system is heavily dependent on the computational model. Physical parameters like coil geometry, input current, and testing apparatus all play a role in the collection of data from a constructed coil. As the primary aim of this project is to evaluate the accuracy of the FEM model in comparison to a physical system, it is important that these factors are thoroughly considered and that the constructed coil sufficiently matches the digitally modeled coil. Because of this, only the single coil and dual coil models will be constructed and the viability of the FEM model assessed before pursuing the Polywell design.

While the construction methods will differ between the single coil and dual coil designs, the same type of data must be collected from each. As previously stated, this will be done through the use of a Vernier Magnetic Field Hall-Effect Sensor which reports β values ranging from 0.32 mT and 6.4 mT. This sensor was chosen because of its integration with other data collection tools and flexible sensor tip which allows fine placement within the coil region. Early tests helped define the testing current for the coils as the models predicted β values outside of the measurable range for the sensor.

To help with data collection, a testing structure will be constructed to allow vertical and rotational travel for the sensor. The sensor structure will be made from acetal homopolymer and fastened using using GO2 Loctite glue. This is done in order to reduce the external effects of metals that cause variances in the μ_2 constant throughout the system. Initially metal screws will be used to fasten the structure while the glue sets, but will be removed during data collection. During data collection, the sensor will be pivoted at an angle of 0 - 50° in steps of 2° while the height is kept constant for each trial. The sensor angle will be validated through the use of external measuring tools. After the data for β against θ is collected, θ will then be converted to the (z, r) coordinate scheme. This conversion can be seen in Figure 1. The height, z, will vary from test to test but will be recorded as well.

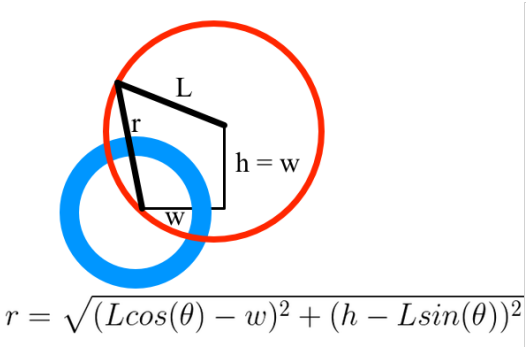

Figure 1: Conversion from offset radial to radial coordinates

3.3 Single Coil Model

The first of the three systems analyzed will be the single coil model. The single coil is most basic of the three systems and does not involve multiple β field interactions. In essence, the single coil system will be primarily the validating the most basic aspects of the FEM model. By testing a single coil first, specific testing procedures can be refined and the mesh model can be further developed without introducing unnecessary complexity.

Several design factors were initially considered in developing the computational model for the single coil system. First, coil geometry like inner and outer

radii, revolved profile, and associated fixtures were considered. A primary factor in designing this specific coil was size and efficiency. Because the β field is constant throughout the center of a solenoid, there will be no difference in β measurements between a large and small coil. Therefore, the smallest coil radius with respect to available materials was selected at 5.08 cm (2.00 inches) and a coil thickness of 2.54 cm. The coil shell will be 3D printed using ABS plastic and will be 3.0mm thick to provide support when winding the wire. These parameters were entered into the SOLIDWORKS design and the 3D model was generated. From the dimensioned profile, an estimate of 275 turns will be required to complete the coil profile with a requirement of 85.6 meters of enameled 16 gauge copper wire.

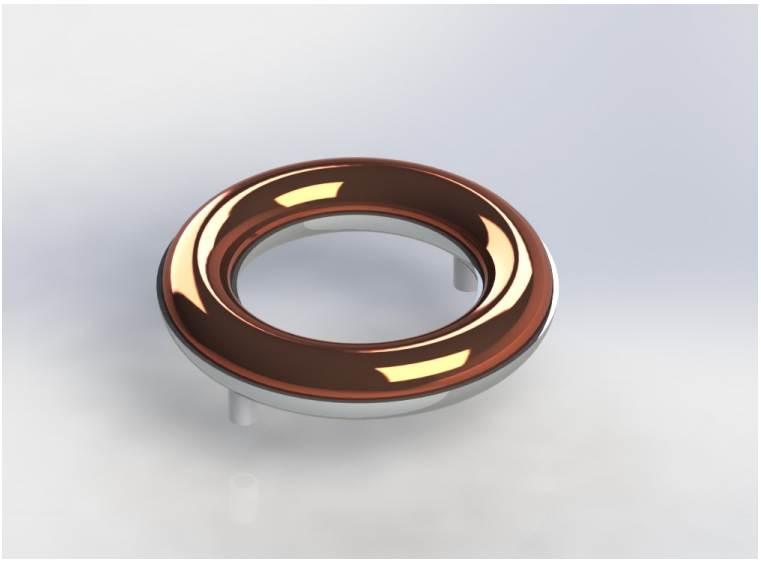

Figure 2: 3D Model of the Single Coil System

3.4 Biconic Cusp Model

The second system analyzed will be the biconic cusp model with an emphasis on β field interactions along and near the ring cusp. This is a higher level test for the FEM model as multiple cusps and a single null point will be formed in the region between both coils. The approach for analyzing the biconic cusp system was slightly different than the single coil system. The single coil system tested the FEM's iterative capabilities where the dual-coil system will be testing the accuracy of the FEM model in specific configurations. Therefore, a magnetic force experiment kit comprised of two Helmholtz coils will be used as a physical device. The computational model will be derived from the specifications of the coils and then validated against data collected from physical testing. In

this test, the physical model will effectively serve as the control and the finite element model is what will be verified.

For this test, it is important to collect β field data in the main regions of interest. These include along the plane between the two Helmholtz coils, the center of said plane, and along the vertical axis of the coils at different radii. The Helmholtz coil pair to be used consists of two 7.0cm mean diameter coils spaced 7.0cmm apart with 168 turns of 18 awg copper wire per coil.

Figure 3: Helmholtz Coil Pair for Biconic Cusp Model

3.5 Polywell Model

Of the three systems presented in this project, the Polywell model is the most conceptual. Validations of the FEM model in the single and dual coil tests will help verify the Polywell model and its representation of a quasi-spherical electron confinement device. The Polywell model will consist of six coils following the same specifications as outlined in the single coil section. Each coil will be spaced

6.35 mm (.25") from eachother at the tangent edges. The regions of interest will include the null point, lines along a corner point cusp, and edge point cusp, and a central point cusp as well as the strength of the β fields around the null point. One interesting aspect to explore will be how the strength of the magnetic field affects the size of the null point.

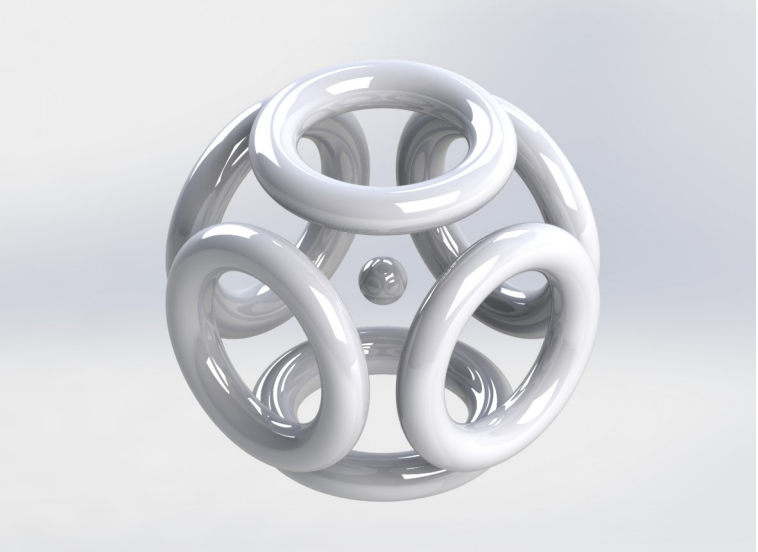

Figure 4: 3D Model of the Polywell System

4 Data

4.1 Single Coil Model

The finite element analysis was run with a "semi-fine" mesh size with 32 mesh units per solid body diagonal. This resulted in 871,265 mesh elements and 145,349. The overall mesh tolerance was 1.69e-003 inches and took 36 seconds to calculate. Shown in Figure 11, the maximum β field achieved was 8mT located within the coil at r = 2, 1 cm above the coil surface. In FEM, this value is measurable, however it is not in measurable on the physical model as the data point is located just slightly inside the coil. In total, 20 data points were collected ranging from an r of 0 to 16.5 cm for each height above the coil. Values on plane with the coil were not collected as they would be immeasurable with the physical system. The data for each height and r is shown in Figure 11

4.2 Single Coil Physical System

The raw data for the physical single coil system is presented below in Figure 5. This is in the format of β vs θ. For analysis, these data will be converted from

offset radial coordinates to coil-centered radial coordinates using the formula described in Figure 1. This set of data represents three independent trials at an operating current of 2.01 amps with a measured coil resistance of 1.8 ohms. Initially, the trial was conducted at an operating current of 3.00 amps, but the strength of the magnetic field exceeded the 6.4 mT capabilities of the hall magnetic field probe. This required the change from 3.00 amps to 2.00 amps, but it should be noted that a coil strength of greater than 6.4 mT at 3.00 amps is desirable for a system where nuclear-fusion level magnetic confinement occurs in the 1 Tesla range. The data presented in Figure 5 does not include any sort of filtering or systematic adjustments.

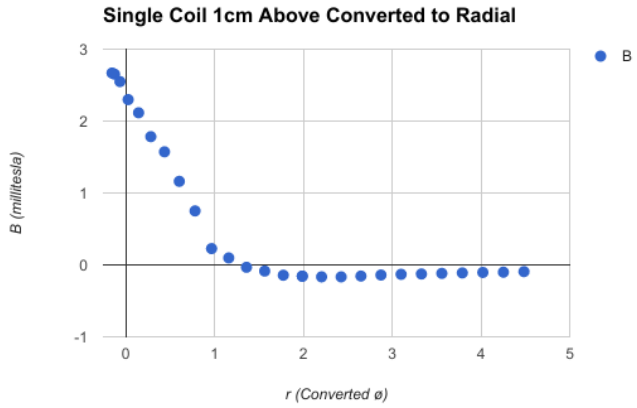

Figure 5: Physical Model Single Coil Data

4.3 Dual Coil Model

The dual coil model was much more in-depth and more complicated to model and mesh than the single coil model. A total of 2,498,965 mesh elements comprised the biconic cusp system and took a time of 4 minutes and 48 seconds to solve. Once again, a "semi-fine" mesh size was used, but on relatively smaller solid bodies increasing the overall accuracy of the model. This is evident as the tolerances were even tighter for the dual coil over the single coil system with a margin of error of 1.55e-3 in per mesh unit.

4.4 Dual Coil Physical System

Data of the β fields were collected for the Helmholtz dual coil physical system. Two types of trials were performed, one where the hall probe was inserted into the central dividing plane, perpendicular to the solenoid axis, and one where the probe was inserted down into the region of space between the coils. This allowed

for the collection of data in separate axes to analyze the null point geometry. The combined field interactions are well represented in Figure 6 where the field strength increases as the coil is inserted into the system, and then drops to 0 where a magnetic null point is formed.

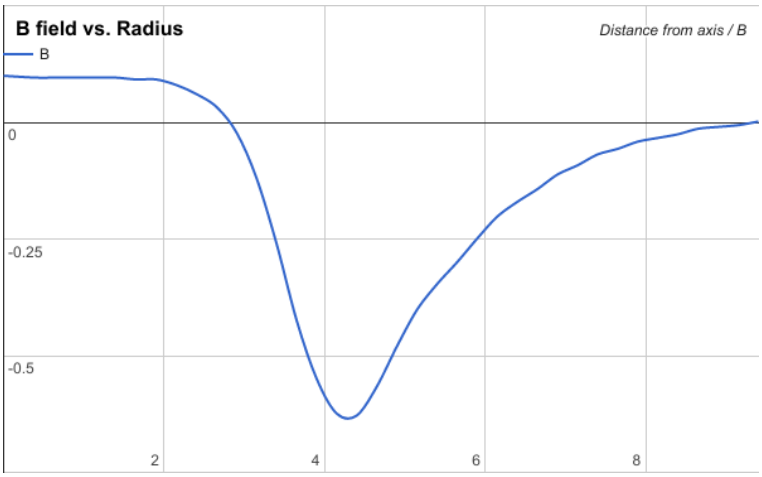

Figure 6: Helmholtz Midplane Insertion Data

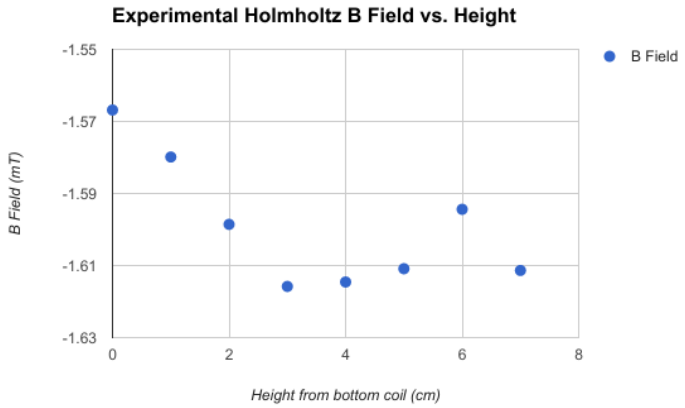

Figure 7: Helmholtz Vertical Insertion Data

5 Analysis

5.1 Single Coil

The single coil model and experimental system followed a similar trend in β values as function of distance away from the radial axis. One major difference between the model and the physical system was the lack of β field reduction as the coil passed over one edge of the coil. The experimental data suggested that the magnetic field within the coil region remained constant while the computational data suggests that at low enough z values (height), the β field will begin to decrease perpendicular to the central axis. This is likely because the magnetic field vectors begin to change orientation when close enough to the inner diameter. The revolve profile for the single coils is unique in that it employs a round bobbin. The round bobbin profile does not generate a flat and uniform field, so field analysis and interactions will not be linear. These round shapes are responsible for cusp formation in magnetic mirror configurations and play a major role in maintaining the "wiffle-ball" style electron trap as discussed earlier.

One major finding of the computational model was the lack of magnetic penetration and relative compactness of the β field around the coil. The vector field model demonstrates relatively high magnetic field above and below the coil rather than around it. According to the data, the physical model is underperforming the computational model by about 1 millitesla directly above the mean coil diameter. During construction of the physical coil, it was noted that despite the number of turns being the same for the both systems, the physical model did not completely fill the volume of the ABS shells, leading to less present magnetic field at the edges ofthe coil body. According to the computational model, this represents about 0.5-1.0 cm radius difference, not including the 3mm thickness of the shell. It is possible that the enameling for the magnet wire was thinner than previously thought, allowing for tighter packing and a reduced coil profile size. In addition, the coil was wound using a winding jig, but did have angled winds nearing the end of the wire length. These nonuniform winds can be responsible for an out-of-round magnetic field which is not easily detectable with the (z, r) coordinate scheme.

Despite these setbacks, the finite element model and physical device produce similar trends in the reduction of the β field strength with a period of medium reduction, high reduction, and low reduction as r increases. This analysis is derived through visual comparison of the experimental and computational data.

5.2 Dual Coil

The dual coil system proved to be much more interesting to model and mesh. As the focus was primarily on interactions of the β fields along the dividing plane, the meshing process had to accommodate 0-length vectors as shown in a round-profile coil biconic cusp simulation in Figure 8. The round profile biconic cusp simulation utilized the same coils from the single coil system and a spacing equal

to the mean coil diameter, similar to the Helmholtz coils in the magnetic force kit. A direct contrast can be made among the computational and experimental data for the Helmholtz coils and the round profile biconic cusp. The Helmholtz coils produce a null point, but this can not be proven the the vertical insertion test. In Figure 7, a vertical change of 7 cm within the two fields only produces a variance of .0477 m which does not fit the finite element model and traditional particle in cell models of magnetic null points.

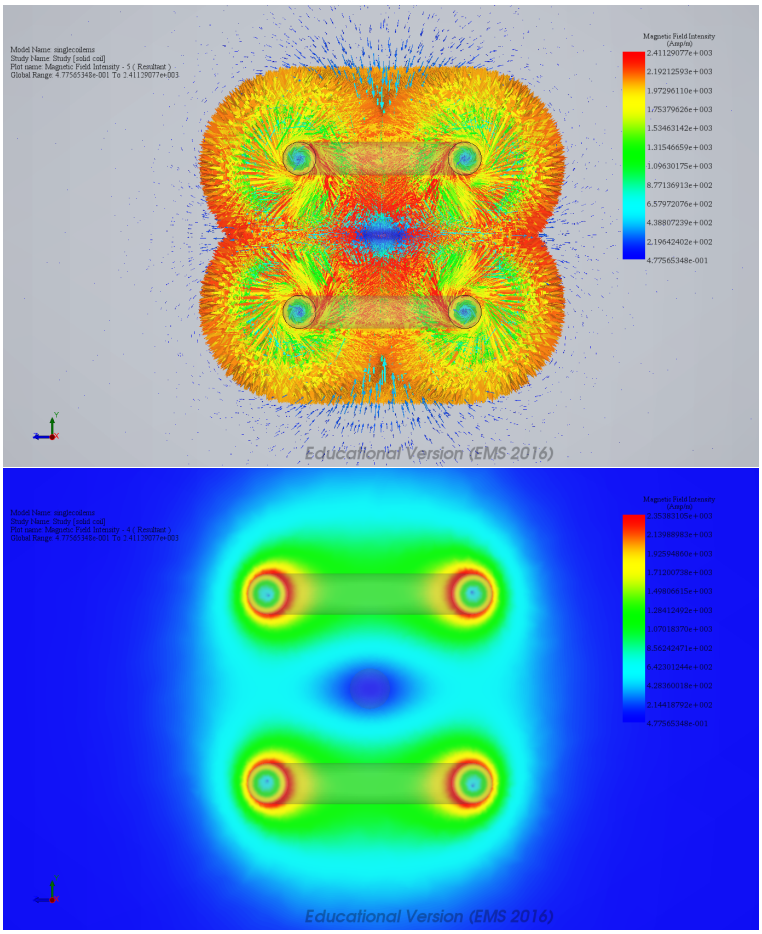

Figure 8: Physical Model Single Coil Data

The midplane insertion test does indeed fit the finite element model of β fields approaching a magnetic null point. In both the experimental (Figure 6) and computational models (Figure 9), the magnetic field is 0 at r = 0, and increases quickly before dropping off as r exceeds the coil major radius. In addition, the computational model suggests that by increasing the operating current, dB will initially be greater and generate a more compact confinement

region.

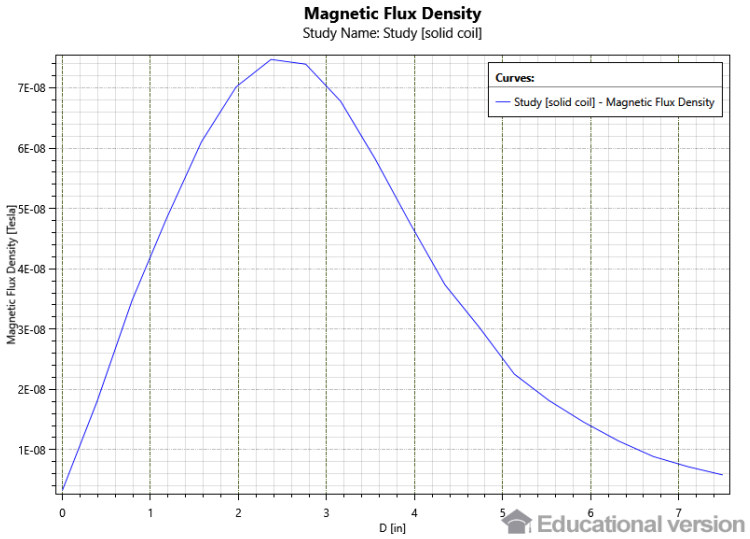

Figure 9: Physical Model Single Coil Data

6 Conclusions

After an in-depth analysis and comparison of both the computational and experimental data, several conclusions can be drawn about the use of the Finite Element Method in modeling β field interactions and coil design. As the current Polywell and biconic cusp systems remain unoptimized in design, new methods of analyzing electromagnet coil design must be implemented with the ability to quickly iterate design geometry. Traditional particle in cell calculations are effective at analyzing given parameters, but are not suited for the iterative design process in the way that Finite Element Analysis is.

This study provided experimental data for a computational method that shows promise in optimizing inertial electrostatic fusion coil design and system geometry with the intent to produce sufficent electrostatic and magnetostatic fields for break even energy generation.

The experimental single coil demonstrated similar β field behavior to the respective computational model, however initial approximations of coil packing were slightly off and the magnetic field was reduced near the edges of the coil. Future work with the single coil design would be to create a "packing profile" that is integrated with the 3D printed shell, ensuring that every coil would be constructed exactly to the 3D modeled specifications. This would not only increase the accuracy of the physical model, but allow very high levels of repeatability necessary for use in biconic and quasi-spherical cusp geometries.

The dual coil experiment produced β field data very similar to that of the finite element model. This is extremely promising for nuclear fusion coil geometry design where accurately modeling β field interactions are key to successfully trapping electrons and forming a potential well. Because the experimental data supported the finite element model so well, the finite element model can continue to be used to analyze the wide variety of cusps for complex geometry like the Polywell.

Despite the effectiveness of the FEM model in solving β fields, there were several issues that must be addressed before truly validating its use in designing inertial electrostatic fusion coils. First, there were major differences between the true magnetic field values for FEM model and the experimental coils. This made numerical analysis of the two sets of data difficult as standard tests for variance would simply fail to produce statistical evidence that the FEM model was statistically similar to the experimental coil, despite similar behaviors. In addition, the complex behavior of the β fields along cusps and in the magnetic null point result in similar statistically insignificant results simply because of data collection offsets and imperfect coil design.

The method of collecting data using the pivoting hall sensor was also slightly flawed. A fairly complicated conversion formula is required to transcribe θ values into the (z, r) coordinate format, and produces a variable rate of radius change. This is undesirable as the θ values must be calculated by hand, introducing a layer of innaccuracy to the data.

Overall, this project provides a framework for future work involving the finite element method and calculating β fields around coils for use in inertial electrostatic confinement fusion. The FEM model will be invaluable in generating coil geometry quickly which can then be passed off to particle in cell simulations that determine the properties of the confined plasma. The next step of this research is to analyze the viability of the FEM model for use in the Polywell system and to model the complex cusps and plugging methods using the electrostatic solvers.

References

[1] J. Berkowitz et al. "Cusped geometries". In: *Journal of Nuclear Energy (1954)* 7.3-4 (1958), pp. 292–293. DOI: 10.1016/0891-3919(58)90159-1. URL: http://www-naweb.iaea.org/napc/physics/2ndgenconf/data/Proceedings%5C%201958/papers%5C%20Vol31/Paper23_Vol31.pdf.

[2] Krall Bussard R. W. *Electron Leakage Through Magnetic Cusps in the Polywell Confinement Geometry.* Tech. rep. Aug. 1991.

[3] W. Bussard and Katherine E. King Emc. *Bremsstrahlung Radiation Losses in Polywell Systems.* Tech. rep. Aug. 1991.

[4] V. Bychkov, M. Modestov, and C.K. Law. "Combustion phenomena in modern physics: I. Inertial confinement fusion". In: *Progress in Energy and Combustion Science* 47 (2015), pp. 32–59. ISSN: 0360-1285. DOI: http://dx.doi.org/10.1016/j.pecs.2014.10.001. URL: http://www.sciencedirect.com/science/article/pii/S0360128514000665.

[5] Matthew Carr et al. "Low beta confinement in a Polywell modelled with conventional point cusp theories". In: *Physics of Plasmas* 18.11 (2011), p. 112501. DOI: 10.1063/1.3655446. URL: https://drive.google.com/file/d/0B1__jpGiM_HNN0VkTy0wdzJoOGs/view?usp=sharing.

[6] M. Khachan Cornish S. Gummersall. "The dependence of potential well formation on the magnetic field strength and electron injection current in a polywell device". In: *Physics of Plasmas* 21 (9 Sept. 2014). DOI: 10.1063/1.4894475.

[7] T J Dolan. "Magnetic electrostatic plasma confinement". In: *Plasma Physics and Controlled Fusion* 36.10 (1994), p. 1539. URL: http://stacks.iop.org/0741-3335/36/i=10/a=001.

[8] EMC2. "Method and apparatus for controlling charged particles". US20080187086A1. 2008.

[9] David V. Gummersall et al. "Scaling law of electron confinement in a zero beta polywell device". In: *Physics of Plasmas* 20.10 (2013), p. 102701. DOI: 10.1063/1.4824005. eprint: http://dx.doi.org/10.1063/1.4824005. URL: http://dx.doi.org/10.1063/1.4824005.

[10] John Hedditch, Richard Bowden-Reid, and Joe Khachan. "Fusion energy in an inertial electrostatic confinement device using a magnetically shielded grid". In: *Physics of Plasmas* 22.10 (2015), p. 102705. DOI: 10.1063/1.4933213. URL: http://scitation.aip.org/content/aip/journal/pop/22/10/10.1063/1.4933213.

[11] A. S. Kaye. "Plasma losses through an adiabatic cusp". In: *Journal of Plasma Physics* 11 (01 Feb. 1974). DOI: 10.1017/s002237780002448x.

[12] J D Lawson. "Some Criteria for a Power Producing Thermonuclear Reactor". In: *Proceedings of the Physical Society. Section B* 70.1 (1957), p. 6. URL: http://stacks.iop.org/0370-1301/70/i=1/a=303.

[13] A. Mahdavipour B.Salar Elahi. "New results on structure of low beta confinement Polywell cusps simulated by comsol multiphysics". In: *Results in Physics* 6 (2016), pp. 873–876. DOI: 10.1016/j.rinp.2016.11.003. URL: http://dx.doi.org/10.1016/j.rinp.2016.11.003.

[14] Massimiliano Mattei, Carmelo Vincenzo Labate, and Domenico Famularo. "A constrained control strategy for the shape control in thermonuclear fusion tokamaks". In: *Automatica* 49.1 (2013), pp. 169–177. ISSN: 0005-1098. DOI: http://dx.doi.org/10.1016/j.automatica.2012.09.004. URL: http://www.sciencedirect.com/science/article/pii/S0005109812004657.

[15] Jef Ongena and Yuichi Ogawa. "Nuclear fusion: Status report and future prospects". In: *Energy Policy* 96 (2016), pp. 770–778. ISSN: 0301-4215. DOI: http://dx.doi.org/10.1016/j.enpol.2016.05.037. URL: http://www.sciencedirect.com/science/article/pii/S0301421516302658.

[16] Todd H. Rider. "A general critique of inertial-electrostatic confinement fusion systems". In: *Physics of Plasmas* 2.6 (1995), pp. 1853–1872. DOI: 10.1063/1.871273. eprint: http://aip.scitation.org/doi/pdf/10.1063/1.871273. URL: http://aip.scitation.org/doi/abs/10.1063/1.871273.

[17] M. Sadowski. "Plasma confinement with spherical multipole magnetic field". In: *Physics Letters A* 25.9 (1967), pp. 695–696. ISSN: 0375-9601. DOI: http://dx.doi.org/10.1016/0375-9601(67)90480-X. URL: http://www.sciencedirect.com/science/article/pii/037596016790480X.

[18] M. Sadowski. "Plasma containment in a spherical multipole magnetic trap". In: *Journal of Plasma Physics* 4.1 (Feb. 1970), pp. 1–12. DOI: 10.1017/S0022377800004773. URL: https://www.cambridge.org/core/article/div-class-title-plasma-containment-in-a-spherical-multipole-magnetic-trap-div/B0B8BBD596D9B66ADD0D37FB41E43324.

[19] *The Advent of Clean Nuclear Fusion Superperformance Space Power and Propulsion*. Vol. 57. International Astronautical Congress. IAF IAA, 2009.

[20] Balasubramanian Viswanathan. "Chapter 6 - Nuclear Fusion". In: *Energy Sources*. Ed. by Balasubramanian Viswanathan. Amsterdam: Elsevier, 2017, pp. 127–137. ISBN: 978-0-444-56353-8. DOI: http://dx.doi.org/10.1016/B978-0-444-56353-8.00006-X. URL: http://www.sciencedirect.com/science/article/pii/B978044456353800006X.

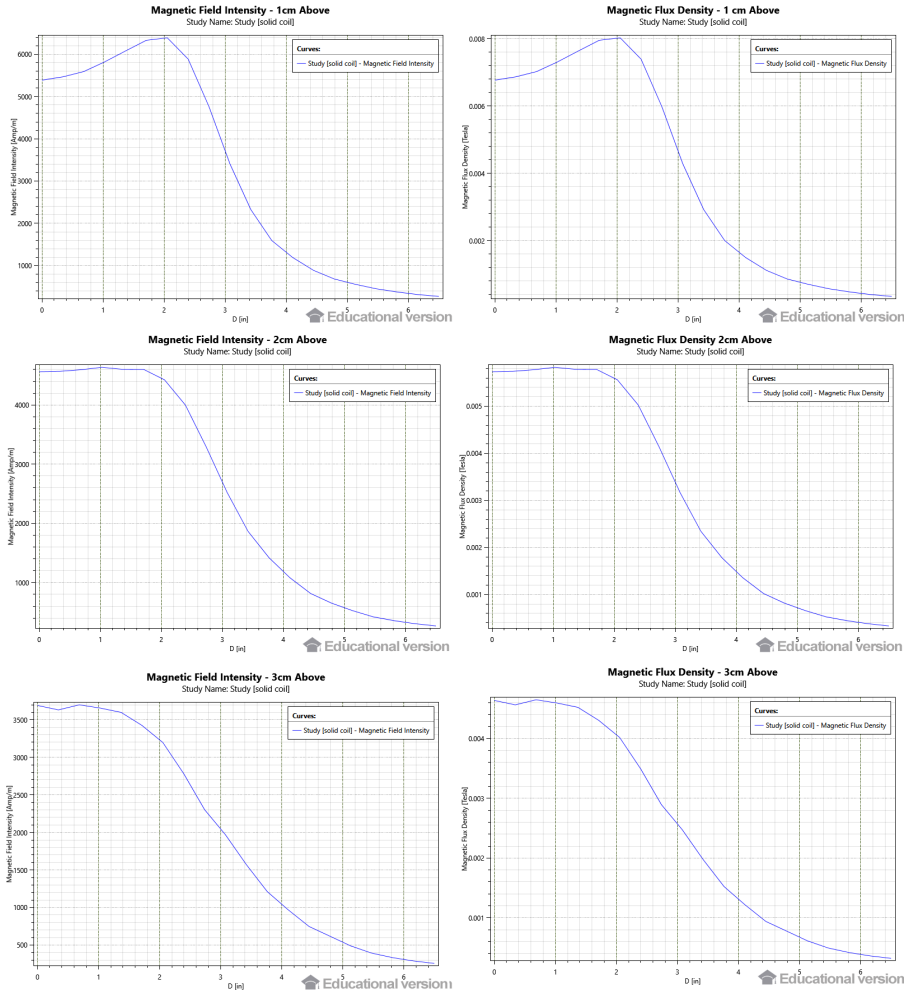

Figure 10: Raw Data for the Single Coil Model

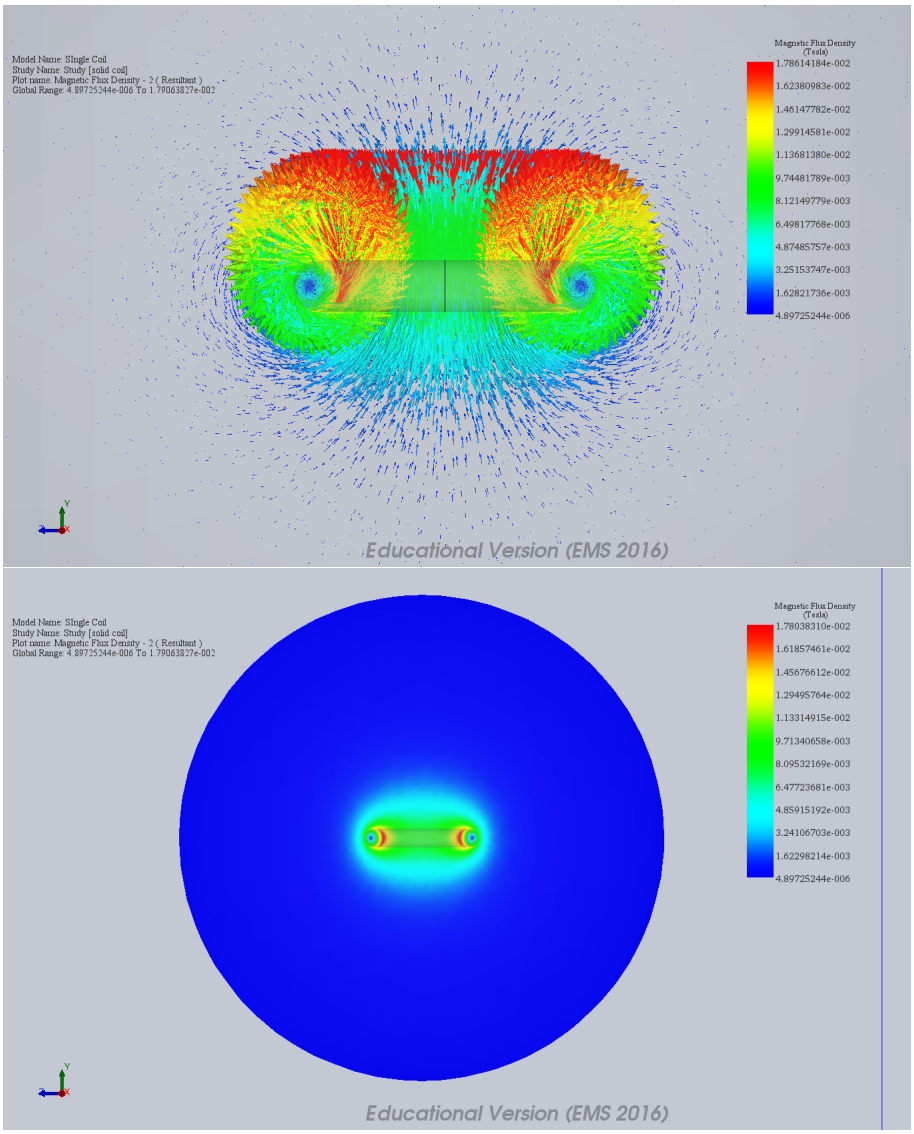

Figure 11: Vector field and fringe plot of single coil system